Earthquake Engineering, Tenth World Conference © 1992 Balkema, Rotterdam. ISBN 90 5410 060 5

Simulation analyses on the shaking table test of scaled BWR model

Katsuya Igarashi & Norio Inoue
Kajima Technical Research Institute, Kajima Corporation, Japan

Hideki Morishita & Noriyoshi Nakamura
Tokyo Electric Power Company, Japan

Norio Suzuki
Kobori Research Complex, Kajima Corporation, Japan

ABSTRACT: Simulation analyses are conducted on the results of a shaking table test of the 1/12 scale BWR full model using two analytical models. One is the model that is used in the actual design. It does not have the hysteresis loop and its damping factor is given in advance. The other is a new developed model that has the hysteresis loop, whose damping factor increases automatically depending on the damage of the model. The dynamic responses of the test structure from weak to strong nonlinear range are simulated quite well. The practicality of the analytical models adopted is confirmed through these simulation analyses.

1 INTRODUCTION

The shaking table test of the 1/12 scale model of BWR Mark II reactor building was carried out as seen in Yano(1989). The test structure was subjected to the consecutive input of earthquake motion from low to destructive level. The test structure was demolished with the shear failure on the 3rd floor at the end of test. The purpose of this paper is to establish the analytical model and to confirm the practicality of the model through the simulation analyses on the test results.

2 ANALYTICAL MODEL

The test structure is the 1/12 scale model of the BWR mark II type reactor building as shown in Fig.1.

Eliminating the complexity of the actual building and neglecting the soil structure interaction, the prototype structure was redesigned. Then it was scaled down to 1/12 to comply with the law of similarity and the limitation of the shaking table.

Compressive strength of concrete is 23.5MPa, and total weight of the test structure is approximately 5MN.

2.1 *The flexure-shear type lumped mass model*

The test structure was idealized to the 13 masses 3-sticks flexure-shear type lumped mass model as shown in Fig.2 based on the method proposed by Tanaka(1986).

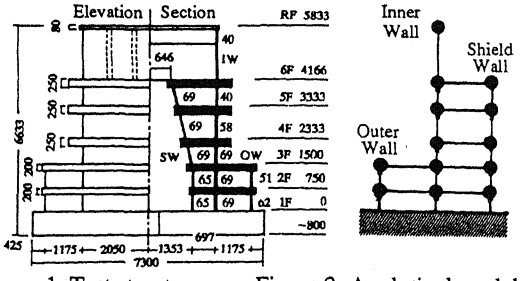

Figure 1. Test structure Figure 2. Analytical model

The validity of the flexure-shear model was already confirmed by comparing with the results of FEM analytically, but it has not been confirmed experimentally.

Inside the wall of the test structure, strain gauges were placed in a shape of triangle. Shear stress of wall was measured using the Mohr's circle as explained in Fig.3.

Shear force acting on each wall was estimated by multiplying the shear stress with the shear area of the wall. The apportionment of the shear forces acting on each wall system was calculated by 14 low level tests and compared with the analytical results as shown in Table 1.

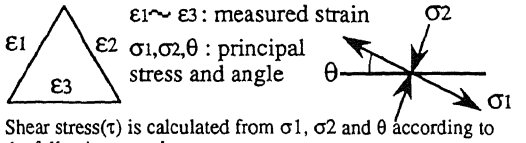

Shear stress(τ) is calculated from σ1, σ2 and θ according to the following equation

$\tau = 0.5(\sigma 2 - \sigma 1)\sin(2\phi)$; where $\phi = 270° - \theta$

Figure 3. Method of measuring shear stress in wall by triangle shape of strain gauges

Table 1. The apportionment of shear force of each wall

Position		Experiment	Analysis
1st floor	Shield Wall	0.10	0.14
	Inner Wall	0.27	0.35
	Outer Wall	0.63	0.52
2nd floor	Shield Wall	0.14	0.13
	Inner Wall	0.41	0.38
	Outer Wall	0.45	0.49
3rd floor	Shield Wall	0.22	0.21
	Inner Wall	0.78	0.79
4th floor	Shield Wall	0.27	0.20
	Inner Wall	0.73	0.80
5th floor	Shield Wall	0.34	0.16
	Inner Wall	0.66	0.84

On the 1st and the 5th floor, where the boundary condition suddenly change, the differences between analytical and experimental results are large. With the other floors, the analytical and experimental results agree quite well, and the errors are less than 10%.

From those results, it is confirmed that the analytical model adopted here represents the fundamental characteristics of the test structure quite well.

2.2 *Skeleton curve*

Shear force acting on each floor was calculated by multiplying the mass of the floor with the observed acceleration record of the floor, and by accumulating from top to the noticed floor of the test structure. The measurement of the story drift was done only on the 3rd floor. As for other floors, the story drift was calculated by double integrating of the relative acceleration time history.

The accuracy of the calculated story drift was confirmed by comparing the calculated one with the measured one on the 3rd floor. Taking the shear force as the ordinate and the story drift as the abscissa, the load-story drift relationship was obtained on each test. Their Peak points are plotted in Fig.4. The analytical load-story drift relationship of the test structure was calculated using the tri-linear skeleton curves proposed by Tanaka(1987). It was obtained by applying the stepwise increasing static load that was proportional to the 1st mode of the vibration to the model afore mentioned. The results are plotted in Fig.4 in broken line. On the 1st and 2nd floor, the analytical results are slightly smaller than the experimental results, but with the other parts, the analytical results cover the experimental results quite well. The analytical load-story drift relationship of each floor is idealized to the tri-linear skeleton curve that is used in the following analyses.

3. RESTORING FORCE MODEL

The differences of the characteristics of the model, which are the rule of the hysteresis loop and the type of damping factor, affect the analytical results strongly.

Two models are used in the simulation analyses. One is the model conventionally used in the actual design of the nuclear reactor building in Japan, and the other is the model developed in this study.

3.1 *Model used in the actual design (called Model A)*

The hysteresis rule used in this model is shown in Fig.5.

The hysteresis rule for a flexure component is the peak oriented before yield point (My), and there is no hysteresis damping in the loop. After yield point, a stable loop becomes a parallelogram and has a hysteresis damping. The rule for a shear component is a peak oriented and the loop does not have the hysteresis damping.

The analytical deflection of the flexure component is not large enough to exceed the yield point. It means that both the flexure and the shear component do not have any hysteresis damping. On the other hand, an equivalent damping factor obtained by the experiments is the combination of the viscous and the hysteretic damping and is impossible to separate. It increases depending on the damage of the test structure as shown in Fig.6. Therefore all the damping is applied as the viscous type in a priori as shown in Table 2.

The damping matrix is the strain energy proportional type. It is recalculated using the deteriorated stiffness of test structure after an analysis of each test to take into account the degradation of it.

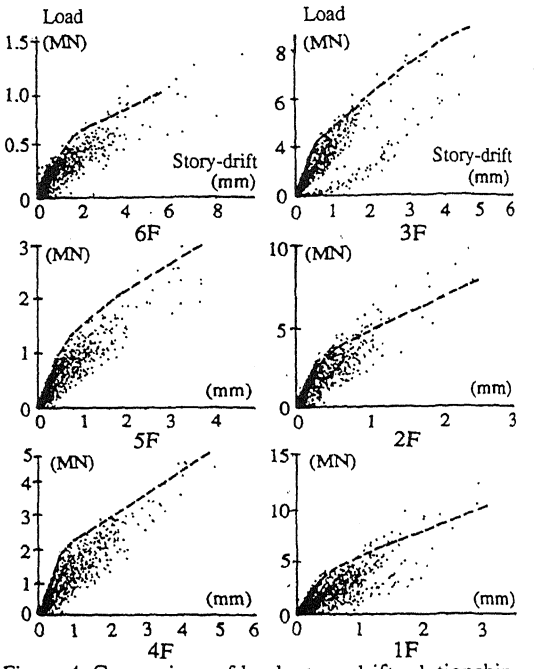

Figure 4. Comparison of load- story drift relationship

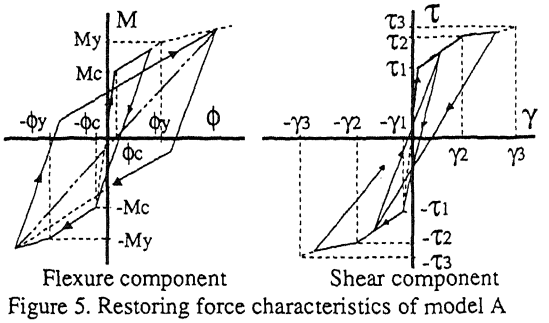

Figure 5. Restoring force characteristics of model A

Table 2. Test case and assumed damping factor

Test name	Observed input Acceleration	Assumed Damping
0.5A0	137 Gal	2 (%)
A0	257 Gal	2 (%)
1.6A0	646 Gal	4 (%)
2.0A0	567 Gal	4 (%)
2.3A0	568 Gal	4 (%)
2.6A0	674 Gal	5 (%)
4.5A0	1247 Gal	6 (%)
6.0A0	1394 Gal	8 (%)
9.0A0	2658 Gal	10(%)

3.2 *New developed model (called Model B)*

The restoring force model is defined with reference to the study of Sato(1989) and Inada(1987) as follows;

1. A stable loop is a parallelogram as shown in Fig.7.
2. The shape of loop is defined by evaluating the interception of the abscissa (a), which is calculated by assuming that the equivalent damping increases depending upon the amount of the story drift.

As mentioned in 3.1, the change of the damping factor with the damage of the test structure is presented in Fig.6. It is assumed that the viscous damping in an elastic range is about 2% and constant. The rest of the damping is assumed to be the hysteresis damping that increases with the increase of story drift.

The relationship between the hysteresis damping and the displacement on shear component is assumed as shown in Fig.8 based on Fig.6 and the work of Sato(1989). The same relationship is applied to the flexure component.

The rules are;

1. It is an elastic range until the 1st break point($\gamma 1$), then the hysteresis damping is zero
2. At $\gamma 2$ point, the apparent damping factor obtained from experiment is 6%. Subtracting the 2% of viscous damping, the hysteresis damping at $\gamma 2$ is 4%. The damping factor varies linearly between $\gamma 1$ and $\gamma 2$.
3. The damping factor is 4% and constant between $\gamma 2$ and $\gamma 3$(4/1000)
4. The damping factor at the final stage is approximately 10% and the shear deformation angle on the 3rd floor is about 8/1000, which is equal to $2\gamma 3$. Subtracting 2% of viscous damping, the equivalent hysteresis damping at $2\gamma 3$ is 8%. The damping factor varies linearly between $\gamma 3$ and $2\gamma 3$.

4. SIMULATION ANALYSIS

Among many tests, major 9 tests are selected as the object of the simulation analysis as shown in Table 2.

Simulation analyses were carried out in the same situation as the actual test sequence to take into account the effect of the previous test. Level A0 in Table 2 produces the response shear stress of 2.35MPa, which is 10% of the compressive strength of concrete at the 3rd floor of inner wall, that is predicted to be the weakest part of the test structure. On this test, level A0 was 275Gal.

In the actual test, the overturning moment of the test structure causes an unfavorable pitching motion of the shaking table. Therefore, to simulate the actual movement of the shaking table, both the horizontal and the pitching acceleration recorded on the base of the test structure were input simultaneously in the analytical model.

4.1 *Results of Simulation analysis*

Among 9 tests shown in Table 2, results of 4 tests that are 2A0, 2.3A0, 4.5A0 and 9A0, are discussed below.

Analytical results of both models are compared with experimental results in the response spectrum at the 6th floor with 1% of the critical damping as presented in Fig.9, and in the profile of the maximum response acceleration distribution as shown in Fig.10. The thick line represents the analytical results and thin line represents the experimental results.

1. In 2A0 test, the test structure went into the plastic range slightly. As for the response spectrum, both models can simulate the peak frequencies of the 1st and the 2nd mode and the twin peaks of the 1st mode. As to the distribution of maximum response value, the analytical results are slightly larger at the 3rd, the 4th and the roof floor, but a good correlation is shown as a whole.

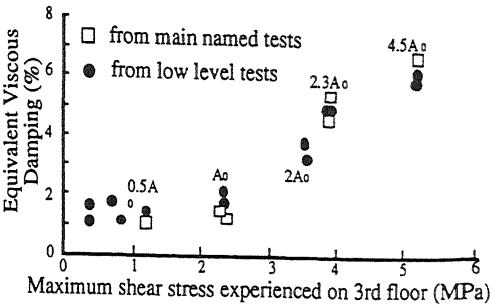

Figure 6. Relationship between equivalent viscous damping & maximum shear stress experienced on the 3rd floor of the inner wall

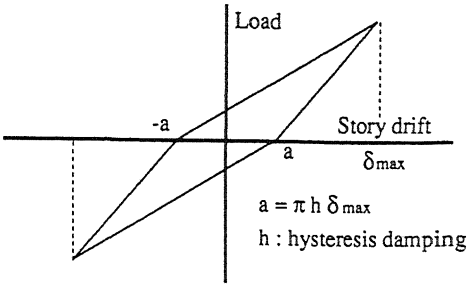

Figure 7. Assumed load-story drift relationship in model B

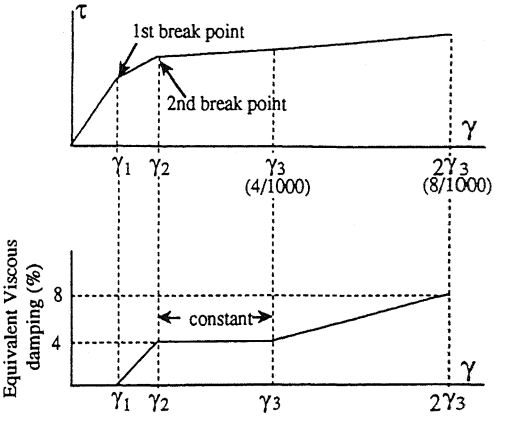

Figure 8. Relationship between assumed restoring force model and equivalent viscous damping

2. In 2.3A0 test, the amplitudes of response spectrum of analytical results are larger than the experimental results, and the peak frequency of the 1st mode is slightly higher. The result of model A shows better correlation than that of model B. As for the distribution of maximum response value, both models show a good correlation with the experimental results.

3. In 4.5A0 test, the 1st and the 3rd floor of the test structure were considerably damaged, so the fundamental characteristics of the test structure were slightly changed. There are some differences in the response spectrum. Model A gives a better correlation than model B. As to the distribution of maximum response value, the results of model A are smaller than the experimental results. Model B shows better correlation than model A.

4. In 9A0 test, the test structure was demolished on the 3rd floor, then the response of the test structure became so complex. As for the response spectrum, model A gives the good correlation on peak frequencies and their amplitudes. Model B gives a good correlation on peak frequencies but gives a larger amplitude. As for the distribution of maximum response value, the results of model A are smaller than the experimental results as a whole. The results of model B show good correlation with the experimental results, except the roof floor.

5. CONCLUSION

With the flexure-shear lumped mass model that is commonly used in the actual design, the fundamental dynamic characteristics of the complex structure like a nuclear reactor building is evaluated precisely.

Simulation analyses are conducted using two analytical models. One is the model that is used in the actual design. It does not have the hysteresis loop, and its damping factor is given in advance. The other is the newly developed model that has the hysteresis loop, whose damping factor increases automatically depending on the damage of the test structure. The dynamic behavior of the test structure from an elastic stage to the collapse stage is traced successfully.

Through the simulation analyses, the practicality of the analytical models adopted in this study is confirmed.

REFERENCES

Inada, Y 1987. Restoring force characteristics of reactor building based on load tests and numerical analysis : Transaction of AIJ No.371, 378 and 382

Sato, S et al 1989. Application of high strength rebar for RC shear wall (part1 to part7): AIJ paper pp. 567--580

Tanaka, H et al 1986. Study on simplified modeling method of wall-type structure: Proc. 7th JEES pp. 1435--1440

Tanaka, H et al 1987. Evaluation method for restoring force characteristics of R/C shear walls of reactor building (part1 to part6): AIJ paper pp 289--300

Yano, Y & K. Hijikata. 1989. Vibration test of a model of nuclear power plant using a large shaking table (part2 BWR 1/12 scale model) : Proc. 9th WCEE Vol. VI pp 735--740.

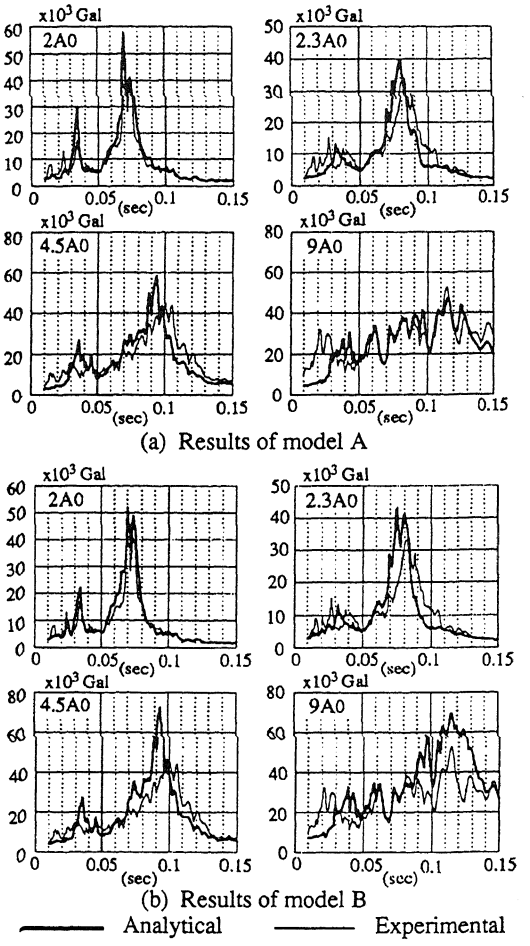

Figure 9. Comparison of acceleration response spectrum on 6th floor (damping 1%)

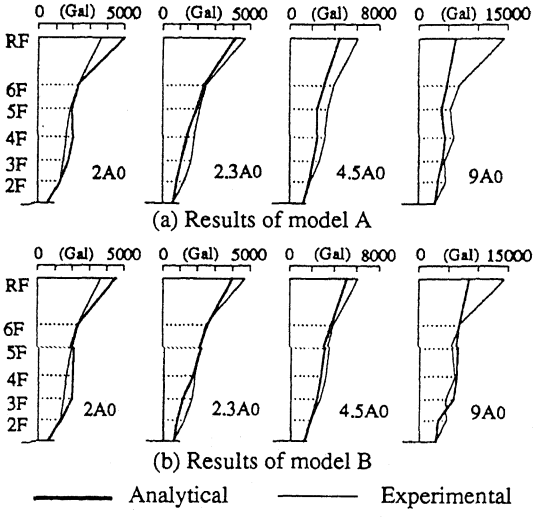

Figre 10. Comparison of the distribution of response maximum acceleration